

# Superplasticity in a 7055 aluminum alloy subjected to intense plastic deformation

R. Kaibyshev, T. Sakai, I. Nikulin, F. Musin and A. Goloborodko

Superplasticity in a 7055 aluminum alloy subjected to intense plastic straining through equal channel angular extrusion (ECAE) was studied in tension over a range of strain rates from  $1.4 \times 10^{-5}$  to  $5.6 \times 10^{-2} \text{ s}^{-1}$  in the temperature interval 300–450°C. The alloy had a grain size of  $\sim 1 \mu\text{m}$ . A maximum elongation to failure of  $\sim 750\%$  occurred at a temperature of 425°C and an initial strain rate of  $5.6 \times 10^{-4} \text{ s}^{-1}$ , with a strain rate sensitivity coefficient  $m$  of about 0.46. The highest  $m$  value was  $\sim 0.5$  at a strain rate of  $1.4 \times 10^{-3} \text{ s}^{-1}$  and  $T \geq 425^\circ\text{C}$ . Moderate superplastic properties with a total elongation of about 435% and  $m$  of  $\sim 0.4$  were recorded in the temperature interval 350–400°C; no cavitation was found. It was shown that the main feature of superplastic behaviour of the ECAE processed 7055 aluminum alloy is a low yield stress and strong strain hardening during the initial stages of superplastic deformation. Comparing the present results with the superplastic behaviour of the 7055 Al subjected to thermomechanical processing (TMP), the highest tensile elongation in the ECAE processed material occurred at lower temperatures because ECAE produces a finer grained structure. MST/5543

Professor Kaibyshev (*rustam@anrb.ru*), Mr Nikulin and Dr Musin are at the Institute for Metals Superplasticity Problems, Khalturina 39, Ufa 450001, Russia. Professor Sakai and Dr Goloborodko are in the Department of Mechanical and Control Engineering, The University of Electro-Communications, Chofu, Tokyo 182-8585, Japan.

## Introduction

The aerospace industry has a great interest in the novel 7055 aluminum alloy (denoted 7055 Al herein) for the fabrication of complex parts due to its high strength combined with sufficiently high fracture toughness, fatigue, ductility and corrosion resistance.<sup>1</sup> These advantages make for efficient application of 7055 Al as a structural material for upper wing elements of airplanes. However, the fabrication of frames and thin walled panels requires enhanced workability, which can be achieved by making this material superplastic. It is known,<sup>2,3</sup> that aluminum alloys having grain sizes less than  $\sim 10 \mu\text{m}$  are capable of achieving high superplastic ductility.

The utilisation of superplastic forming technology in large bulk billets is currently limited because of difficulties in producing ultrafine grain structures.<sup>2</sup> Commercial 7055 Al produced by ingot metallurgy has an average grain size of  $\sim 100 \mu\text{m}$ .<sup>4</sup> A complex thermomechanical processing (TMP) regime was developed recently to achieve superplasticity in this material.<sup>4,5</sup> However, this technique has two important limitations. First, this TMP provides fine grained structure in sheets with a thickness less than 2 mm.<sup>4</sup> Second, this two-step TMP<sup>4,5</sup> resulted in a partially recrystallised structure consisting of larger grains with a size of  $\sim 11 \mu\text{m}$  and recovered subgrains with a mean size of 2  $\mu\text{m}$ . The volume fraction of recrystallised grains was about 64%.<sup>4,5</sup> Therefore, it is necessary to develop a new TMP to produce 7055 Al having a fully recrystallised structure and finer grains.

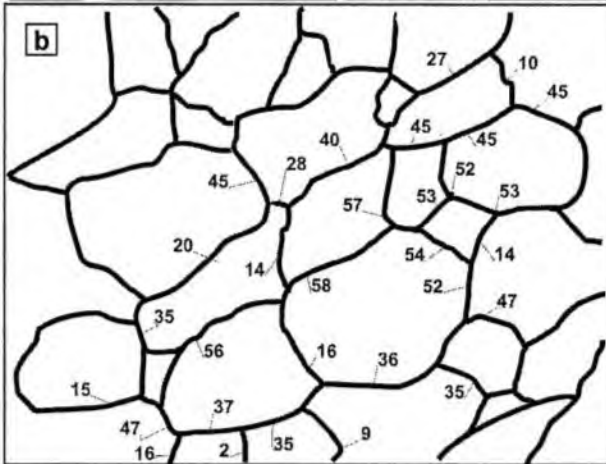
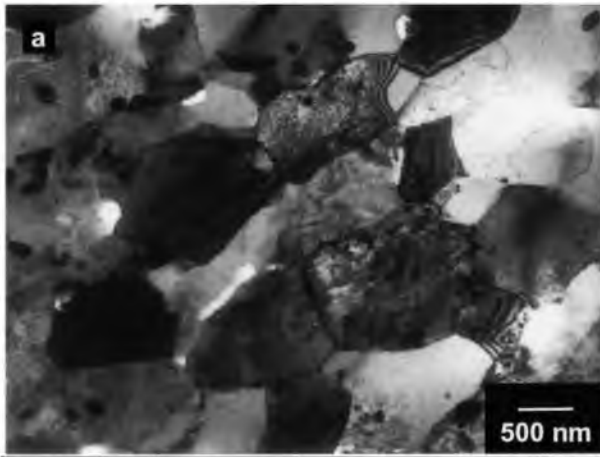
It was shown,<sup>6–8</sup> that equal channel angular extrusion (ECAE) is capable of producing significant grain refinement in aluminum alloys due to the occurrence of dynamic recrystallisation during intense plastic straining in simple shear. Aluminum alloys subjected to ECAE with large strains can exhibit high superplastic properties.<sup>8–10</sup> Thus, the main aim of the present study is to achieve superplasticity in bulk billets of 7055 Al using ECAE processing. There is much interest in the application of moderate strain to produce an ultrafine grain structure in 7055 Al, as this could be extremely important on economic grounds.

The present work is a continuation of studies on 7055 Al, with the intention of evaluating its potential for superplasticity. A second objective is to provide a direct comparison of ECAE and TMP in the development of superplastic capability of 7055 Al.

## Material and experimental procedure

7055 Al with the chemical composition (wt-%) Al–8.2Zn–2.1Mg–2.2Cu–0.2Zr–0.09Mn–0.09Fe–0.07Si–0.04Ni–0.02Ti–0.08Cr was manufactured by direct chill casting and then homogenised at 470°C for 24 h and cooled in air. The surface of the alloy ingot 250 mm in diameter and 1200 mm in height was shaved to remove  $\sim 15$  mm. Bars with dimensions 25 × 25 × 120 mm were machined from the central part of the ingot parallel to the major direction and then ground into rods with diameter 20 mm and length 100 mm. These rods were deformed to a true strain of 4 by ECAE at 300°C by repeated pressing without any rotation of the sample, i.e. route A.<sup>7,8</sup> An isothermal die with a circular internal cross-section and an L shaped configuration with angles  $\phi$  and  $\psi$ ,<sup>6,8</sup> both equal to 90°, was used for the extrusion. Deformation through this die produced a strain of about 1 on each passage.<sup>6–8</sup> Following the ECAE, tensile samples of 6 mm gauge length and 1.4 × 3 mm<sup>2</sup> cross-section were machined from the extruded rods; the tensile axis was parallel to the former extrusion direction of the pressed rods. These samples were tensile tested to failure at temperatures ranging from 300 to 450°C and strain rates ranging from  $1.4 \times 10^{-5}$  to  $5.6 \times 10^{-2} \text{ s}^{-1}$ . Other details of mechanical tests were described in earlier reports.<sup>4,5</sup>

Samples were analysed by optical metallography and transmission electron microscopy (TEM) using procedures given in detail in previous works.<sup>4,5</sup> In the present study, samples tested to failure were sectioned in planes containing the longitudinal (tension) and long transverse directions, and the microstructural evolution was examined under conditions of static annealing in grip sections and dynamic annealing in gauge sections at a strain rate of  $1.4 \times 10^{-3} \text{ s}^{-1}$  in the temperature range 300–450°C. Cavitation was



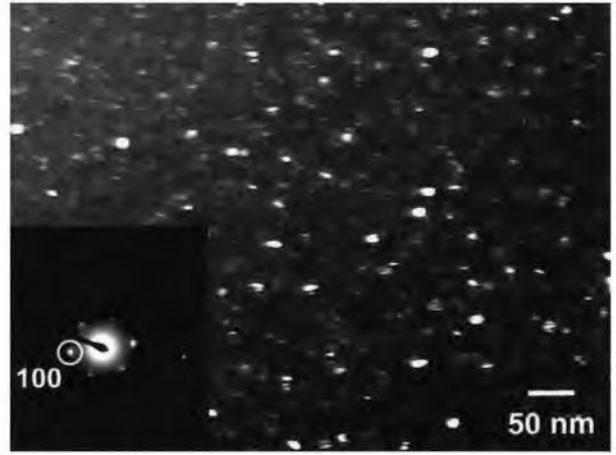
1 Typical ultrafine grained structure in 7055 Al deformed to a strain of about 4 by ECAE processing at 300°C: the numbers represent misorientation angles of boundaries in degrees

examined by a metallography technique and a buoyancy method<sup>11</sup> in samples tested to failure. Misorientations of the grain boundaries induced by the ECAE were analysed using the conventional Kikuchi line technique in TEM. The accuracy of measurements was about 1°. Misorientation analysis was applied to 31 grain boundaries.

## Experimental results

### MICROSTRUCTURE AFTER ECAE

A typical TEM structure of ECAE processed 7055 Al and the corresponding misorientation map are shown in Fig. 1. It is clearly seen that the ECAE at 300°C to a strain of 4 results in the formation of fine crystallites with an average size of  $\sim 1 \mu\text{m}$ . Grain aspect ratio (AR), defined as the ratio of the grain dimension in the longitudinal (extrusion) direction to that in the transverse direction, is close to 1.3. High angle boundaries (HABs) with misorientations over 15° account for 90% of the deformation induced boundaries and, therefore, HABs dominate the resulting structure. Transverse boundaries with low angle misorientation were rarely observed and their fraction is  $\sim 10\%$ . Careful observation of many areas showed that the microstructure of the ECAE processed 7055 Al was reasonably homogeneous, although in some areas the recrystallised structure shown in Fig. 1 alternated with regions of recovered subgrains. The volume fraction of recrystallised regions was over 85%. In the recrystallised regions, the grains outlined by HABs contained a few dislocations in their



2 Dark field image showing distribution of  $\text{Al}_3\text{Zr}$  dispersoids in 7055 Al

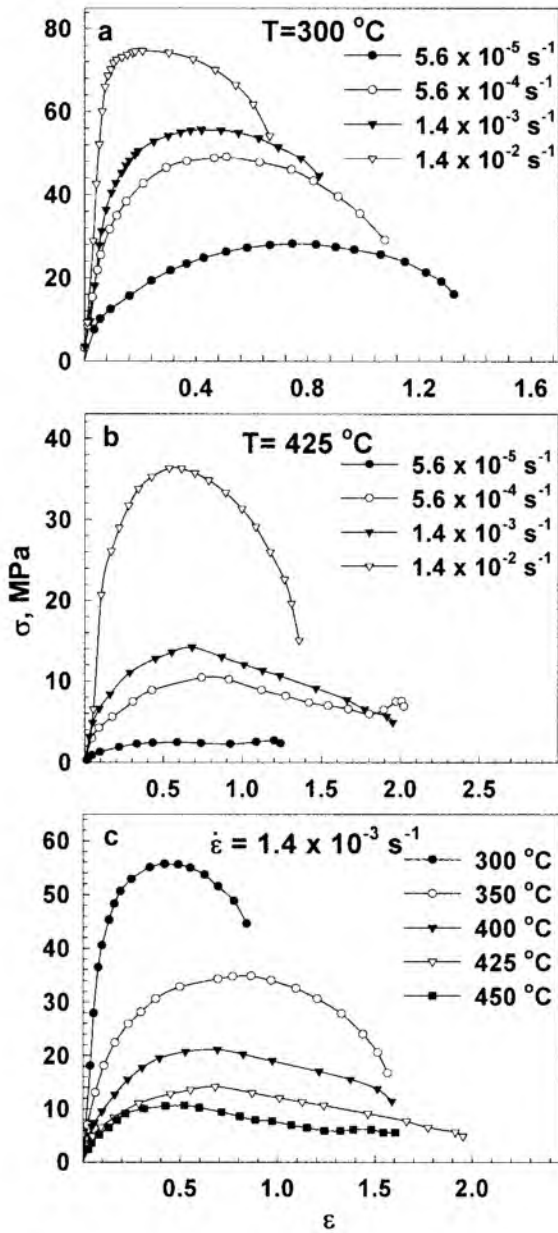
interiors ( $\rho \approx 10^{12} \text{m}^{-2}$ ) but parts of them had moderate dislocation densities.

Inspection of the TEM structure of ECAE processed 7055 Al with a (100) dark field image showed that there was a uniform distribution of  $\text{Al}_3\text{Zr}$  dispersoids having an average size of  $\sim 20 \text{nm}$  (Fig. 2). Examination of a bright field image showed that most of these  $\text{Al}_3\text{Zr}$  dispersoids exhibited incoherent boundaries suggesting a stable structure. The volume fraction of coherent or semicoherent  $\text{Al}_3\text{Zr}$  dispersoids, distinguished by a specific contrast in aluminum matrix near the particles, was found to be about 20% from all of them.

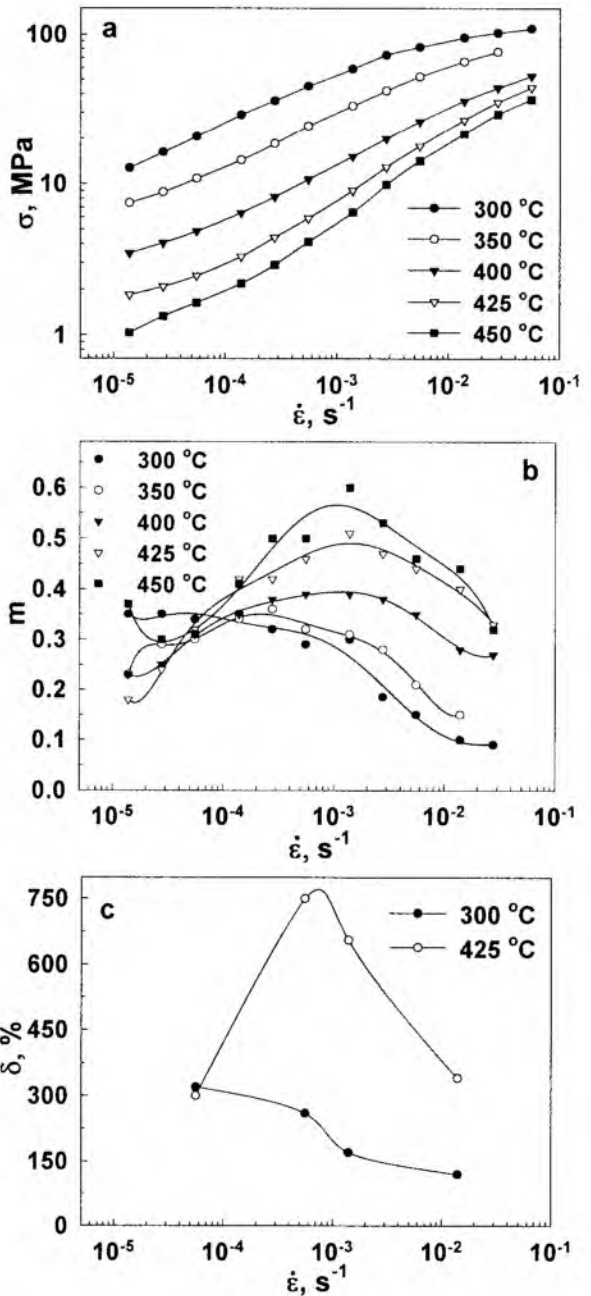
### SUPERPLASTIC BEHAVIOUR

Typical true stress–true strain ( $\sigma$ – $\varepsilon$ ) curves for 7055 Al with ultrafine grain structure are presented in Fig. 3a and b at temperatures of 300°C and 425°C, respectively, over a range of strain rates from  $1.4 \times 10^{-5}$  to  $5.6 \times 10^{-2} \text{s}^{-1}$ . Figure 3c shows the  $\sigma$ – $\varepsilon$  curves at an initial strain rate of  $1.4 \times 10^{-3} \text{s}^{-1}$  and temperatures ranging from 300 to 450°C. It is seen that the flow stress is strongly dependent on strain, which is atypical for superplastic deformation. There is a stress peak at moderate strain. At low temperatures and/or high strain rates, a sharp softening after the stress peak can be attributed to extensive localised necking over the gauge length (Fig. 4). Gradual strain softening after the peak stress tends to appear at higher strains with decreasing strain rate or increasing temperature. An apparent steady state flow can be distinguished at  $T > 400^\circ\text{C}$  and  $\dot{\varepsilon} \leq 5.6 \times 10^{-4} \text{s}^{-1}$ , at which plastic flow over the gauge length was found to be roughly uniform (Fig. 4).<sup>2,3</sup>

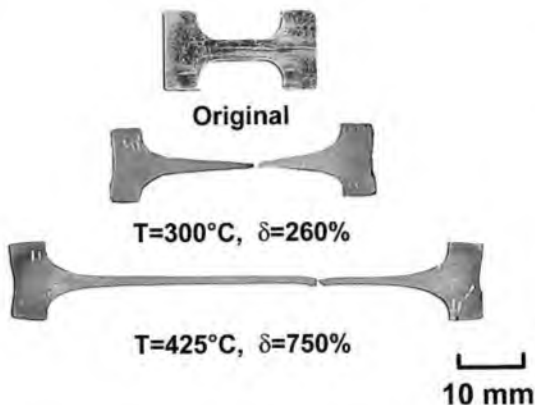
Figure 5a gives a plot of the flow stress taken at  $\varepsilon \sim 0.34$  as a function of initial strain rate on a double logarithmic scale. It is apparent that at  $T \geq 350^\circ\text{C}$ , the  $\sigma$ – $\dot{\varepsilon}$  curves exhibit a sigmoidal shape, as in standard superplastic alloys.<sup>2,3</sup> At 300°C, the highest elongation to failure  $\delta$  of  $\sim 320\%$  (Fig. 5c) and a strain rate sensitivity,  $m \sim 0.34$  (Fig. 5b) were found at  $\dot{\varepsilon} = 5.6 \times 10^{-5} \text{s}^{-1}$ . The  $m$  and  $\delta$  values tend to increase with decreasing strain rate. Increasing temperature leads to the appearance of well defined maximums in  $m$  and  $\delta$  values in the strain rate range  $10^{-4}$ – $10^{-2} \text{s}^{-1}$ , i.e. superplasticity region 2 is clearly distinguished.<sup>2,3</sup> The optimum strain rate for superplasticity, at which the highest superplastic ductilities are observed, shifts to higher strain rates with increasing temperature from 300 to 450°C. At 425°C, the highest elongation to failure of 750% occurs at a strain rate of  $5.6 \times 10^{-4} \text{s}^{-1}$ , corresponding with  $m \sim 0.46$ . In contrast, 7055 Al subjected to two step TMP exhibited no superplasticity at  $T < 400^\circ\text{C}$ ; at higher



3 Typical true stress-true strain curves for 7055 Al alloy subjected to ECAE: strain rate dependence at a  $300^\circ\text{C}$ , b  $425^\circ\text{C}$ ; and c temperature dependence at initial strain rate of  $1.4 \times 10^{-3} \text{ s}^{-1}$



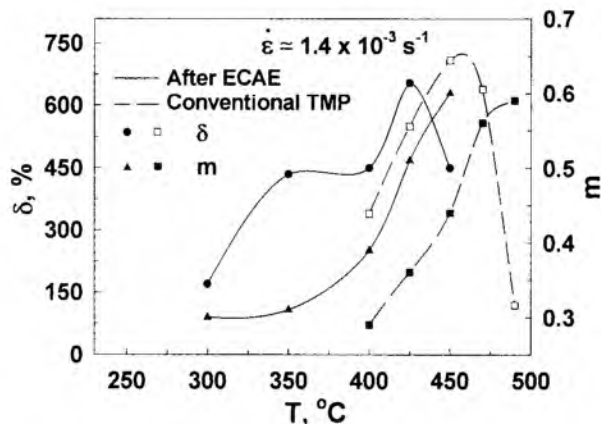
5 a strain rate dependence of flow stress  $\sigma$  at  $\epsilon \sim 0.34$ ; b coefficient of strain rate sensitivity  $m$  at  $\epsilon \sim 0.34$ ; c elongation to failure



4 Untested sample and samples tensile tested to failure at  $\dot{\epsilon}=5.6 \times 10^{-4} \text{ s}^{-1}$

temperatures, the optimum strain rate for superplasticity of  $3.3 \times 10^{-4} \text{ s}^{-1}$  was independent of temperature.<sup>4</sup>

Temperature dependencies of the coefficient of strain rate sensitivity  $m$  and elongation to failure  $\delta$  for 7055 Al subjected to ECAE and also the TMP processed material<sup>4</sup> are shown in Fig. 6. It is seen that the  $\delta$  values of the ECAE processed 7055 Al increases from 170% to 410% as temperature increases from  $300$  to  $350^\circ\text{C}$  whereas the  $m$  coefficient remains virtually unchanged ( $m \sim 0.33$ ). Higher temperatures result in increased the  $m$  values. The temperature dependence of elongation to failure shows a maximum at  $425^\circ\text{C}$ , then  $\delta$  rapidly decreases. It is clearly seen in Fig. 6 that in comparison with TMP the ECAE processing leads to a shift in the temperature domain of superplasticity to lower temperatures, enhancing ductility at  $T \leq 425^\circ\text{C}$ . However, at  $450^\circ\text{C}$ , 7055 Al subjected to TMP exhibits higher superplastic ductility.<sup>4,5</sup> Notably, at



**6** Coefficient of strain rate sensitivity  $m$  and elongation to failure  $\delta$  as functions of temperature at  $\dot{\epsilon} \approx 1.4 \times 10^{-3} \text{ s}^{-1}$ . Data for 7055 Al subjected to two step TMP<sup>4</sup> included for comparison

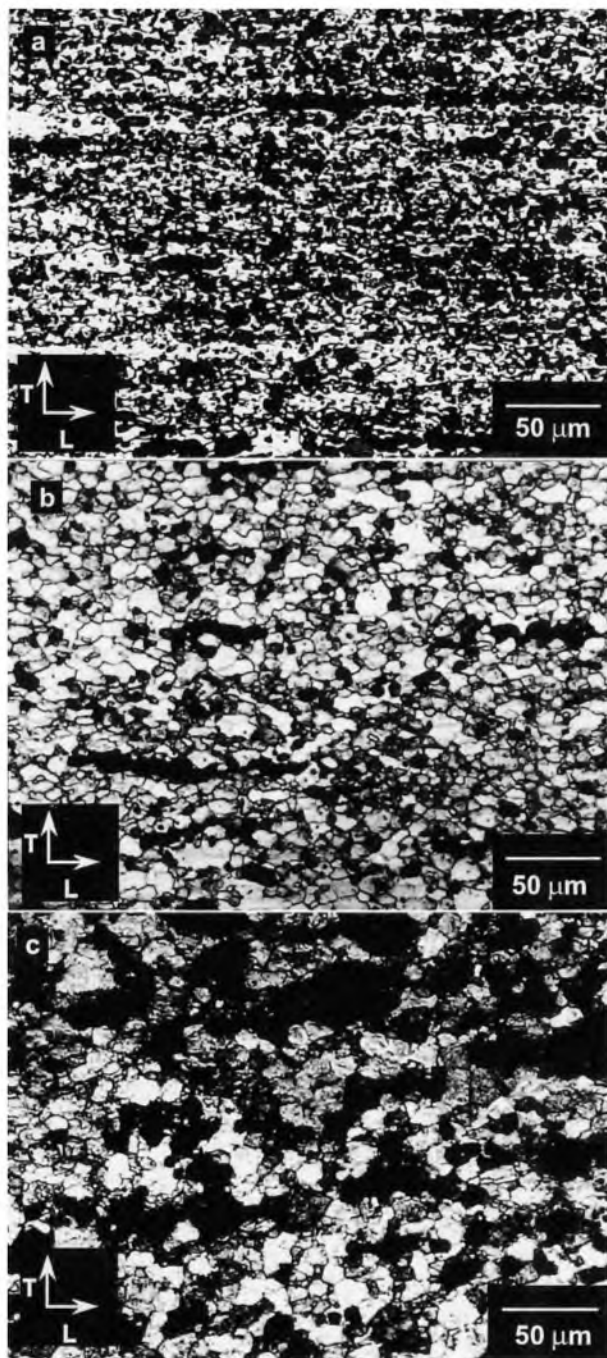
the optimum temperature–strain rate condition the  $m$  value  $\sim 0.5$  is essentially constant over a strain range of 0–1.5 for the ECAE processed material, in contrast with the 7055 Al subjected to two step TMP.<sup>4,5</sup>

## MICROSTRUCTURAL EVOLUTION

Grain sizes developed after static annealing  $L_s$ , dynamic annealing  $L_d$ , and the grain aspect ratio in gauge sections are summarised in Table 1. Under static annealing the initial grains are essentially stable at  $T \leq 350^\circ\text{C}$  and rapidly grow with increasing temperature to  $T \geq 400^\circ\text{C}$  (Table 1). In general, non-uniformity in the structure evolved during ECAE remained under static annealing.

No substantial grain growth takes place during superplastic deformation, and at  $425^\circ\text{C}$ , superplastic deformation leads to an insignificant grain refinement (Fig. 7, Table 1) that can be associated with dynamic recrystallisation. This is generally in contrast with structural changes in standard superplastic materials.<sup>2,3</sup> Superplastic deformation provides uniformity of microstructure (Fig. 7). The volume fraction of unrecrystallised structure decreases with increasing temperature in the range  $300\text{--}400^\circ\text{C}$  (Fig. 7a and b), and at  $425^\circ\text{C}$  the formation of a highly uniform structure consisting of essentially equiaxed grains occurs (Fig. 7b). Grains remain reasonably equiaxed except at  $T = 350^\circ\text{C}$ , where the grain aspect ratio is high (Table 1).

At  $T \geq 400^\circ\text{C}$ , etched cavities were revealed by optical microscopy (Fig. 7b and c). Typical cross-sectional views are shown in Fig. 8. The average size of cavities  $A$ , cavity aspect ratio  $CAR$ , and volume fraction of porosity measured by both the linear intersect method  $V_L$ , and the buoyancy method  $V_B$ , are summarised in Table 2. In the temperature range  $300\text{--}350^\circ\text{C}$  the superplastic deformation induces only limited cavitation. With increasing temperature from  $400$  to  $450^\circ\text{C}$ , the volume fraction of porosity and cavity size strongly increase, approaching  $\sim 10\%$ , suggesting failure caused by cavity interlinkage.<sup>3</sup> Most cavities



a  $T = 350^\circ\text{C}$ ,  $\epsilon = 1.7$ ; b  $T = 425^\circ\text{C}$ ,  $\epsilon = 2$ ; c  $T = 450^\circ\text{C}$ ,  $\epsilon = 1.8$

**7** Microstructures evolved after superplastic deformation at  $\dot{\epsilon} = 1.4 \times 10^{-3} \text{ s}^{-1}$ ; arrows indicate tension (L) and long transverse (T) directions

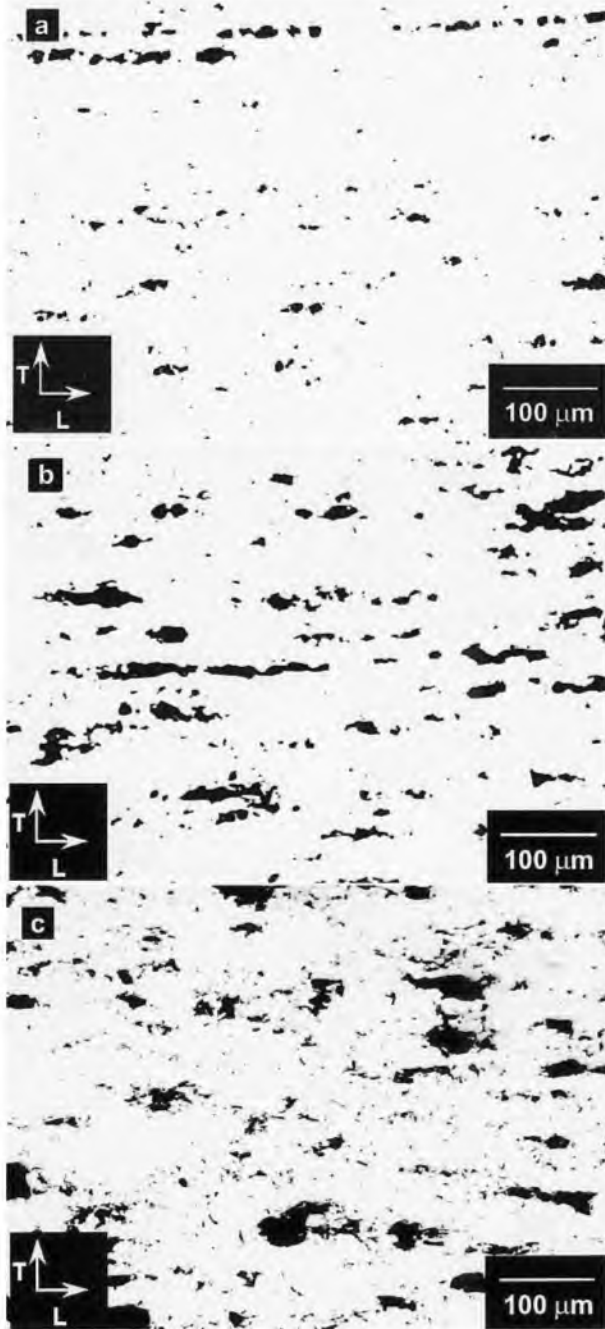
grow along the tensile direction and the average size of cavities  $A$  is roughly similar to that of the dynamic grain size  $L_d$  (see Tables 1 and 2). An irregular and jagged cavity

**Table 1** Average grain size  $L_s$  and  $L_d$  after static annealing and superplastic deformation, and aspect ratio of grains over the gauge section for samples strained to failure at a strain rate of  $1.4 \times 10^{-3} \text{ s}^{-1}$  at different temperatures

$T, ^\circ\text{C}$	300	350	400	425	450
Local strain in gauge section (equivalent time of static annealing in grip section, h)	$\epsilon = 0.9$ (0.87)	$\epsilon = 1.7$ (1.40)	$\epsilon = 1.8$ (1.43)	$\epsilon = 2.0$ (1.83)	$\epsilon = 1.8$ (1.43)
$L_s$ ( $\mu\text{m}$ )	1.4	2.2	5.4	11.4	15.0
$L_d$ ( $\mu\text{m}$ )*	2.0/1.5	2.5/1.6	9.8/8.0	10.9/8.6	15.8/12.0
Aspect ratio	1.30	1.56	1.23	1.26	1.32

\*Numerator and denominator are grain sizes measured in the longitudinal and transverse directions, respectively.





a  $T=400^{\circ}\text{C}$ ,  $\epsilon=1.8$ ; b  $T=425^{\circ}\text{C}$ ,  $\epsilon=2$ ; c  $T=450^{\circ}\text{C}$ ,  $\epsilon=1.8$

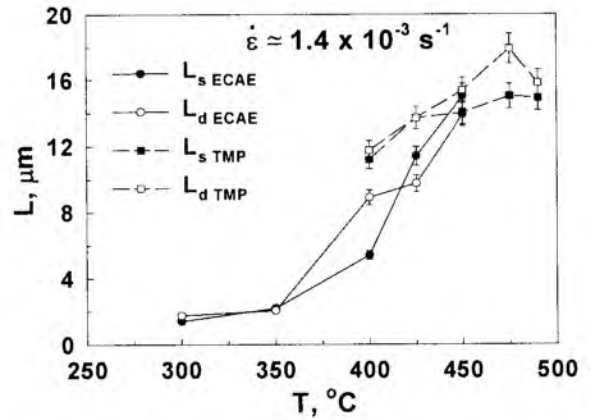
8 Cross-sectional views of samples deformed at  $\dot{\epsilon}=1.4 \times 10^{-3} \text{ s}^{-1}$ . Micrographs taken at position 5 mm from fracture surface. Arrows indicate tension (L) and long transverse (T) directions

Table 2 Average cavity size  $A$ , coefficient of cavity aspect ratio  $CAR$ , and porosity volume fraction for 7055 Al strained at  $\dot{\epsilon}=1.4 \times 10^{-3} \text{ s}^{-1}$  to failure at various temperatures

$T, ^{\circ}\text{C}$	350	400	425	450
$A$ ( $\mu\text{m}$ )*	...	10/8.1	14.4/9.5	17.8/11.1
$CAR$	...	1.2	1.5	1.6
$V_L$ %	...	5.1†	8.7†	8.6†
$V_B$ %	3.6†	6.1†	6.6†	10†

\*Numerator and denominator represent cavity sizes measured in the longitudinal and transverse directions, respectively.

†Values of  $V_L$  and  $V_B$  are for data obtained by metallographic technique and the buoyancy method, respectively.



9 Effect of temperature on static grain size  $L_s$  and dynamic grain size  $L_d$  in 7055 Al alloys subjected to ECAE and TMP<sup>4</sup>

shape may indicate plasticity controlled cavity growth. Cavity interlinkage can result from the formation of cavity chains in the tension direction (Fig. 8a and 8b).

Thus, at  $T < 400^{\circ}\text{C}$ , fracture occurs due to unstable plastic flow.<sup>3</sup> In the temperature interval  $400-450^{\circ}\text{C}$ , the pseudobrittle fracture associated with nucleation, growth, and interlinkage of internal voids takes place.<sup>3</sup>

## Discussion

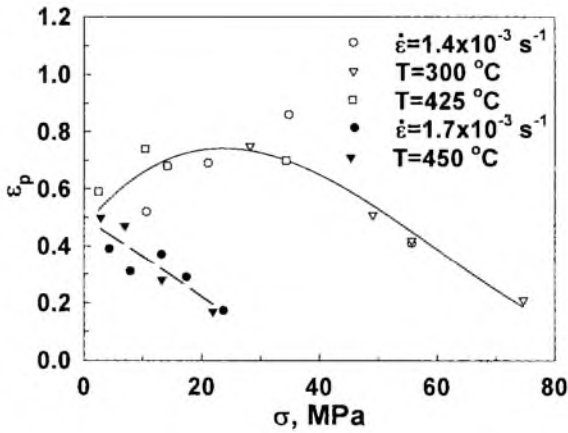
### ACHIEVING SUPERPLASTICITY THROUGH ECAE

The present study demonstrates the feasibility of achieving grain refinement and superplastic ductilities in commercial 7055 aluminum alloy in the as cast condition. This work establishes ECAE as a very effective processing technique to introduce ultrafine grain size ( $\sim 1 \mu\text{m}$ ) into bulk billets of 7055 Al, thereby imposing a moderate true strain of 4 at  $300^{\circ}\text{C}$ . During ECAE processing 7055 alloy behaves as a dilute aluminum alloy in which ultrafine grain structure is developed at a true strain of about 4.<sup>6,7</sup> The presence of incoherent  $\text{Al}_3\text{Zr}$  dispersoids does not lead to a shift of the formation of recrystallised structure to large strain as in Al-Mg-Sc alloys containing coherent  $\text{Al}_3\text{Sc}$  dispersoids.<sup>9,12</sup> The low fraction of  $\text{Al}_3\text{Zr}$  dispersoids could not impede grain boundary mobility and effectively restrict growth of the ultrafine grains only at  $T \leq 350^{\circ}\text{C}$ . As a result, ECAE processed 7055 Al exhibits a maximum elongation to failure of 750% in the recrystallised condition, with a relatively large grain size of  $\sim 10 \mu\text{m}$  at a temperature of  $425^{\circ}\text{C}$ , at which extensive static growth of fine grains takes place. At lower temperatures, the 7055 Al demonstrates marginal superplastic properties.

ECAE processed 7055 Al exhibits an essentially similar maximum elongation ( $\sim 750\%$ ) to TMP processed material ( $\sim 960\%$ ).<sup>4</sup> The highest ductility in ECAE processed 7055 Al occurred at a slightly lower temperature of  $425^{\circ}\text{C}$ , compared with the 7055 Al subjected to TMP ( $450^{\circ}\text{C}$ )<sup>4,5</sup> due to a slightly finer (Fig. 9) and more uniform structure. However, there exist other specific features of superplastic behaviour promoting the use of superplastic forming of ECAE processed 7055 Al.

### CHARACTERISTICS OF SUPERPLASTIC BEHAVIOUR

The most important mechanical characteristic of ECAE processed 7055 Al is its high rate of strain hardening at strains less than the peak strain  $\epsilon_p$  at which the peak stress



10 Relationship between peak strain  $\epsilon_p$  and peak stress  $\sigma_p$  at two constant temperatures and constant strain rate for ECAE processed material (open markers), and at constant temperature and strain rate for TMP processed material (closed markers)<sup>4</sup>

$\sigma_p$  occurs. The  $\epsilon_p$  value increases from  $\sim 0.2$  to  $0.8$  with decreasing  $\sigma_p$  value (Fig. 10). Therefore, at high temperatures and low strain rates there exists a wide strain interval over which extensive strain hardening takes place. ECAE processed 7055 Al exhibits very low values of yield stress (Fig. 3) compared with 7055 Al subjected to two step TMP.<sup>4</sup> An increase in flow stress with strain is normally indicative of strain enhanced grain growth occurring during superplastic deformation.<sup>2,3</sup> However, no significant grain growth was found in the present 7055 Al, even at high strains. It is apparent that extensive strain hardening during the initial stages of deformation is attributable to the high uniformity of ultrafine grain structure. As a result, plastic flow starts at very low applied stress.

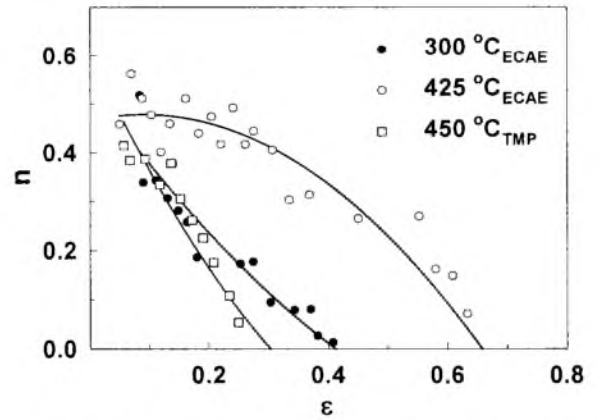
It is known,<sup>3,13</sup> that plastic stability in tension occurs if the value of the sum  $n+m$ , where  $n$  is the strain hardening coefficient and  $m$  is the coefficient of strain rate sensitivity defined by<sup>3,13</sup>

$$\sigma = K \dot{\epsilon}^m \epsilon^n \quad (1)$$

where  $K$  is a constant, is high. The presence of a neck in a material under tension leads to locally high strain rate and increased strain. As a result, for a high value of  $m$  and  $n$ , a sharp increase in flow stress within the necked region occurs, providing resistance to further neck growth. Numerous works<sup>3,3</sup> have demonstrated that if  $n+m > 0.5$ , fracture does not occur due to unstable plastic flow.

Typical dependencies of strain exponent  $n$  on true strain  $\epsilon$  are presented in Fig. 11. It is seen that for  $T < 400^\circ\text{C}$  and  $\dot{\epsilon} \geq 5.6 \times 10^{-4} \text{ s}^{-1}$ , unstable plastic flow ( $n+m < 0.5$ ) (Figs. 5b and 11) takes place, resulting in the material pulling out to a fine 'thread' before failure (Fig. 4). It is apparent that the softening stage under these conditions is the stage of softening associated with extensive necking. In the temperature interval  $400-450^\circ\text{C}$  a value for the sum  $n+m > 0.5$  confers stable plastic flow. At  $\epsilon \leq \epsilon_p$ , superior stability of superplastic flow associated with high strain hardening takes place over a wide strain range (Figs. 10 and 11). This is necessary to manufacture thin walled components using 7055 Al. At  $\epsilon > \epsilon_p$  an  $m$  value of  $\sim 0.5$  is sufficient to provide stable plastic flow.<sup>3,13</sup> In this temperature range the softening stage is associated with the development of cavitation damage.<sup>3</sup> Therefore, highly stable plastic flow at  $T \geq 400^\circ\text{C}$  is provided by the high value of sum  $n+m$  for  $\epsilon < \epsilon_p$  and high  $m$  value for  $\epsilon > \epsilon_p$ .

Furthermore, the ECAE processed 7055 Al exhibited a higher strain hardening coefficient than the 7055 Al subjected to TMP at the initial stages of superplastic deformation. In addition, the coefficient of strain sensitivity



11 Effect of true strain  $\epsilon$  on strain hardening coefficient  $n$

$m$  was virtually independent of strain. The ECAE processing method is, therefore, attractive because the technique has the potential for making large bulk billets of 7055 Al superplastic, and provides enhanced stability of plastic flow in 7055 Al, that is important for fabrication of aviation components with complex shape requiring high formability.

## Conclusions

1. A cast 7055 aluminium alloy with an initial grain size of  $\sim 100 \mu\text{m}$  was subjected to ECAE processing at a temperature of  $300^\circ\text{C}$  to a strain of  $\sim 4$ , thereby reducing the grain size to  $\sim 1 \mu\text{m}$ . Ultrafine ( $\leq 2 \mu\text{m}$ ) and fine ( $\leq 10 \mu\text{m}$ ) grain sizes were retained at temperatures as high as  $350^\circ\text{C}$  and  $425^\circ\text{C}$ , respectively.

2. Moderate tensile elongations of  $\leq 435\%$  were recorded in ECAE processed 7055 Al in the temperature range  $300-400^\circ\text{C}$ . A maximum of elongation to failure of  $750\%$  was found at a temperature of  $425^\circ\text{C}$  and an initial strain rate of  $5.6 \times 10^{-4} \text{ s}^{-1}$  with a corresponding strain rate sensitivity coefficient of about  $0.46$ .

3. A high value of strain hardening coefficient  $n$  at  $\epsilon \leq 0.8$  is a feature of the superplastic behaviour of ECAE processed 7055 Al.

## Acknowledgements

This work was supported in part by the International Science and Technology Center under Project no. 2011. One of the authors (AG) would like to thank the Ministry of Education, Science, Sports and Culture of Japan for scholarship.

## References

1. I. N. FRIDLINDER: *Met. Sci. Heat Treat.*, 2001, **1**, 5–9.
2. O. A. KAIBYSHEV: 'Superplasticity of alloys, intermetallics, and ceramics', 316; 1992, Berlin, Springer Verlag.
3. J. PILLING and N. RIDLEY: 'Superplasticity in crystalline solids', 214; 1989, London, The Institute of Metals.
4. R. KAIBYSHEV, T. SAKAI, F. MUSIN, I. NIKULIN and H. MIURA: *Ser. Mater.*, 2001, **45**, 1373–1380.
5. R. KAIBYSHEV, A. GOLOBORODKO, F. MUSIN, I. NIKULIN and T. SAKAI: *Mater. Trans.*, 2002, **43**, 2408–2414.
6. F. J. HUMPHREYS, P. B. PRANGNELL, J. R. BOWER, A. GHOLINIA and C. HARRIS: *Philos. Trans. R. Soc. (London)*, 1999, **357**, 1663–1681.
7. S. FERRASE, V. M. SEGAL, K. HARTWIG and R. GOFORTH: *Mater. Trans. A*, 1997, **28A**, 1047–1057.

8. Z. HORITA, M. FURUKAWA, M. NEMOTO and T. G. LANGDON: *Mater. Sci. Technol.*, 2000, **16**, 1239–1245.
9. M. FURUKAWA, A. UTSUNOMIYA, K. MATSUBARA, Z. HORITA, M. NEMOTO and T. G. LANGDON: *Acta Mater.*, 2001, **49**, 3829–3838.
10. R. GRIMES, R. J. DASHWOOD, A. W. HARRISON and H. M. FLOWER: *Mater. Sci. Technol.*, 2000, **16**, 1334–1339.
11. R. KAIBISHEV, F. MUSIN, D. GROMOV, T. G. NIEH and D. LESUER: *Mater. Sci. Technol.*, 2003, **19**, 483–490.
12. Z. HORITA, M. FURUKAWA, M. NEMOTO, A. J. BARNES and T. G. LANGDON: *Acta Mater.*, 2000, **48**, 3633–3640.
13. J. W. EDINGTON, K. N. MELTON and C. P. CUTLER: *Prog. Mater. Sci.*, 1976, **21**, 67–170.